B. Gao, H. Fan and X. Zhang,
S. Afr. J. Chem., 2012, **65**, 125–130,
<http://journals.sabinet.co.za/sajchem/>.

Hydrothermal synthesis of $CdWO_4$ nanorods and their photoluminescence properties

Bin Gao[a,b], Huiqing Fan[a,*] and Xiaojun Zhang[b]

[a]*State Key Laboratory of Solidification Processing, School of Materials Science and Engineering, Northwestern Polytechnical University, Xi'an 710072, China.*

[b]*School of Science, Xi'an Polytechnic University, Xi'an 710048, China.*

Received 5 May 2012, revised 28 May 2012, accepted 4 June 2012.

ABSTRACT

$CdWO_4$ nanorods with wolframite structure were synthesized in the presence of the surfactant SDBS by a hydrothermal method, and characterized by a variety of techniques. The obtained products are $CdWO_4$ nanorods with length of 0.8–2.5 μm and width of 50–250 nm. The surfactant SDBS plays a key role in the formation of the $CdWO_4$ nanorods. The pH value impacts on crystallinity of the products. The PL properties of the $CdWO_4$ nanorods prepared under different conditions were studied. The intensity of the PL emissions of the samples increases with crystallinity and aspect ratio of the $CdWO_4$ nanorods.

KEYWORDS

$CdWO_4$ nanorods, photoluminescence, hydrothermal method.

1. Introduction

Tungstates, with high luminescence efficiency, great density, strong resistance to radiation damage, no deliquescence etc., have good application prospects in many fields[1–7]. One phase of $CdWO_4$ belonging to the monoclinic crystallographic system, has a wolframite structure.[8] The lattice constants are a = 0.5029 nm, b = 0.5859 nm, c = 0.5074 nm, β = 91.47 °, respectively.

$CdWO_4$ has a high refractive index, a high X-ray absorption coefficient, low radiation damage, high luminescence intensity and low afterglow to luminescence, and as such is considered a promising light-emitting material. One application of $CdWO_4$ is that it is used as a popular X-ray scintillator at room temperature. $CdWO_4$ scintillators, with high efficiency, short decay time, high stopping power and high chemical stability, etc., are difficult to replace by other scintillators in this field.[9]

As an important luminescent material, $CdWO_4$ crystals were synthesized and their luminescence properties have been studied by many research groups. Up to now, the synthesis methods of $CdWO_4$ mainly include Czochralski's method,[10] molten salt whisker growth technology,[11] high temperature solid state reaction method,[12] laser pulse ablation,[13] spray pyrolysis,[14] sol-gel method[15] and hydrothermal process.[16] Most of the aforementioned synthesis methods can only obtain macro-size $CdWO_4$, and these synthesis processes require high temperature and, hence, are difficult to control. Photoluminescence properties of solid materials are closely associated with size, morphology and micro-structure of the solid light-emitting particles. Therefore, exploring the synthesis of $CdWO_4$ nanocrystal with a special morphology is of important significance to investigating its photoluminescence properties and applications. Compared with other synthetic methods, the hydrothermal approach needs a low reaction temperature, simple operation and facile control composition. This paper reports the synthesis of $CdWO_4$ nanorods through a hydrothermal treatment process using $Na_2WO_4{\cdot}2H_2O$ and $CdCl_2{\cdot}2.5H_2O$ as main raw materials in the presence of sodium dodecyl benzene sulfonate (SDBS) surfactant. The formation mechanism and photoluminescence properties of the synthesized $CdWO_4$ nanorods were studied.

*To whom correspondence should be addressed. E-mail: hqfan3@163.com

2. Experimental

All the chemical reagents used were of analytical grade (Xi'an Chemical Reagent Co. Ltd) and used without further purification. A typical experimental process is described as follows: 2 mmol (0.66 g) of sodium tungstate dihydrate ($NaWO_4{\cdot}2H_2O$) was dissolved in 20 mL de-ionized water in a glass beaker and stirred with a glass rod until the formation of a saturated solution. A certain amount of sodium dodecyl benzenesulfonate (SDBS) was added to the saturated solution under vigorous magnetic stirring. Stirring was continued until a homogeneous solution was formed. 20 mL of a 0.1 mol L^{-1} solution of cadmium dichloride ($CdCl_2{\cdot}2.5H_2O$) was added, drop-wise, to the above-mentioned mixed homogeneous solution while stirring vigorously. The solution immediately became a white opaque suspension. The pH value of the suspension was adjusted with 1 M hydrochloric acid or sodium hydroxide.

The pH value was measured using a pH meter. The final concentrations of SDBS in the solution were 0.005, 0.01 and 0.015 mol L^{-1}, respectively. After 60 min of stirring, the final non-transparent suspension was transferred to a 100 mL Teflon-lined stainless steel autoclave to about 80% of its capacity. The autoclave was sealed and maintained at 180 °C for 24 h and then cooled to room temperature naturally. After the hydrothermal treatment a white precipitate formed at the bottom of the autoclave. The precipitate was centrifuged, filtered, and rinsed with distilled water and absolute alcohol several times to remove any ions possibly remaining in the final products. Finally, the products were dried at 80 °C for 6 h in air to give pale yellow powders.

The crystal structures of the obtained products were recorded on an X-ray powder diffractometer (XRD; D/Max-2400, Rigaku, Tokyo, Japan) with Cu$K\alpha$ radiation (λ = 0.15418 nm). The XRD data were collected over a 2θ range from 15 ° to 80 ° at a scanning rate of 5 ° min^{-1}. The morphologies and microstructures of the synthesized samples were characterized using high-resolution transmission electron microscopy (HRTEM; JEM-3000F, JEOL, Tokyo, Japan), equipped with selected area electron diffraction (SAED) and energy dispersive X-ray spectrometer (EDX; X-Max, Oxford Instruments, Oxfordshire, UK) and operated at 200 kV.

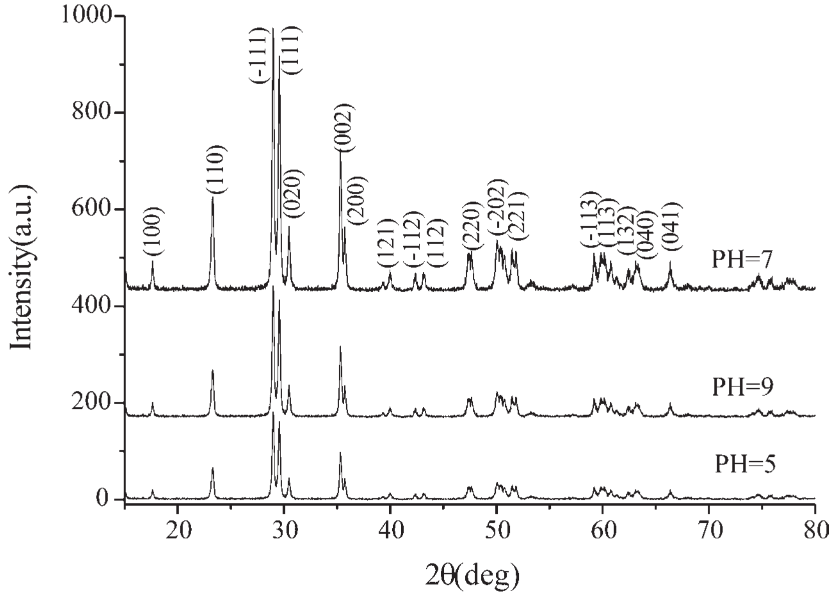

Figure 1 XRD patterns of the $CdWO_4$ nanorods synthesized at 180 °C for 24 h at different pH values.

The photoluminescence (PL) spectra were measured at room temperature on a steady-state fluorescence and phosphorescence lifetime spectrometer (FLSP 920, Edinburgh Instruments Ltd, Livingston, UK) with an excitation wavelength of 320 nm. The excitation source was a steady-state Xe-arc lamp with an output power of 450 W.

3. Results and Discussion

X-ray powder diffraction analysis was employed to determine the crystal structure of the synthesized $CdWO_4$ nanorods. Figure 1 shows the XRD patterns of the $CdWO_4$ nanorods prepared in 0.01 mol L^{-1} SDBS at pH values of 5, 7 and 9. In three cases all the diffraction peaks could be indexed to a pure monoclinic phase of crystallized $CdWO_4$ with a wolframite structure. The calculated cell parameters were a = 0.5021 nm, b = 0.5872 nm and c = 0.5076 nm, which is consistent with the standard values for monoclinic phase $CdWO_4$ (JCPDS, No. 14-0676, a = 0.5029 nm, b = 0.5859 nm, c = 0.5074 nm). No characteristic peaks from impurities were detected by XRD, indicating that the products were highly pure phases. The sharp diffraction peaks indicate that well-crystallized $CdWO_4$ crystals can be obtained under current synthetic conditions.

XRD analysis also showed that the intensity of XRD diffraction peaks of the $CdWO_4$ nanorods obtained at pH of 7 reached a maximum value, suggesting that this condition is the optimal condition for synthesis of crystalline $CdWO_4$ nanorods. The relatively broad peaks probably arise from the small width of the synthesized $CdWO_4$ nanorods.

The morphology of the products was characterized by transmission electron microscopy (TEM). TEM images of samples prepared at 180 °C for 24 h with an SDBS concentration of 0.005, 0.01 or 0.015 mol L^{-1}, are shown in Fig. 2a–c (pH = 7). The TEM images indicate that the products are composed of large-scale nanorods. The TEM observations also demonstrate that an almost 100% yield of $CdWO_4$ nanorods can be easily obtained using this simple method. The nanorods synthesized with an SDBS concentration of 0.005 mol L^{-1} exhibit a narrow distribution of widths ranging from 50 to 80 nm. The lengths of the nanorods are in the order of 800–1300 nm. The nanorods are straight and have smooth, round tips (Fig. 2a). The products obtained with the SDBS concentration of 0.01 mol L^{-1} are shown in Fig. 2b. While the widths of the nanorods are independent of the SDBS concentration, the lengths increase to 1.5~2 μm. At an SDBS concentration of 0.015 mol L^{-1} both the widths and lengths of the nanorods increased compared to the first two products (Fig. 2c). In this case, the widths ranged from 130 to 250 nm and the lengths up to 2.5 μm. It can be seen from the aspect ratio that the $CdWO_4$ nanorods accrete with an increase in the SDBS concentration from 0.005 to 0.01 mol L^{-1}, but decreases when the $SDBS^{-1}$ concentration further raises to 0.015 mol L^{-1}. The aspect ratio of the $CdWO_4$ nanorods prepared in 0.01 mol L^{-1} SDBS is approximately 40. Figure 2d is a selected area, electronic diffraction (SAED) pattern, of a $CdWO_4$ nanorod. The diagram shows clear diffraction spots, indicating that well-crystallized $CdWO_4$ nanorods are single crystals.

The surfactant, SDBS, plays an important role in the formation of the $CdWO_4$ nanorods. In the reaction system, the concentration of the SDBS is larger than its critical micelle concentration (CMC, 1.48 mmol L^{-1}) and so is present in the form of rod-like micelle. There is water in the rod-like micelles and these can be seen as micro-reactors. In the beginning, the ion of WO_4^{2-} is mainly located in the inner surface of the micelle. After adding $CdCl_2{\cdot}2.5H_2O$ solution to the mixture, the Cd^{2+} ions combine with WO_4^{2-} to form $CdWO_4$ crystal. The micelle wrapping limit the crystallization of $CdWO_4$ in a relatively small spatial scale and then inhibit the crystal growth. The micellar shape changes with the SDBS concentration, consequently, $CdWO_4$ nanorods with different morphology are obtained. In addition, the SDBS can be ionized to form dodecylbenzene sulfonic ions (DBS^-) with a different spatial structure. The DBS^- can selectively adsorb onto certain crystal faces of the $CdWO_4$, and thereby decrease the surface energy and growth velocity of these planes in the hydrothermal process. In this way, the $CdWO_4$ crystal nucleus orients growth along a certain direction to form a rod-like structure. The inhibition of the crystal face growth along a particular directions enhances with concentration of SDBS and therefore the growth trend of the grain in a certain direction is more obvious. Thus the aspect ratio of the $CdWO_4$ nanorods increases with SDBS concentration. However, the growth of the $CdWO_4$ crystal in all directions is simultaneously suppressed when the concentration of the SDBS exceeds a certain value. It decreases the aspect ratio of the $CdWO_4$ nanorods. The analysis shows that the surfactant of SDBS in the formation of the $CdWO_4$ nanorods mainly plays the roles of a soft template and an adsorbent.

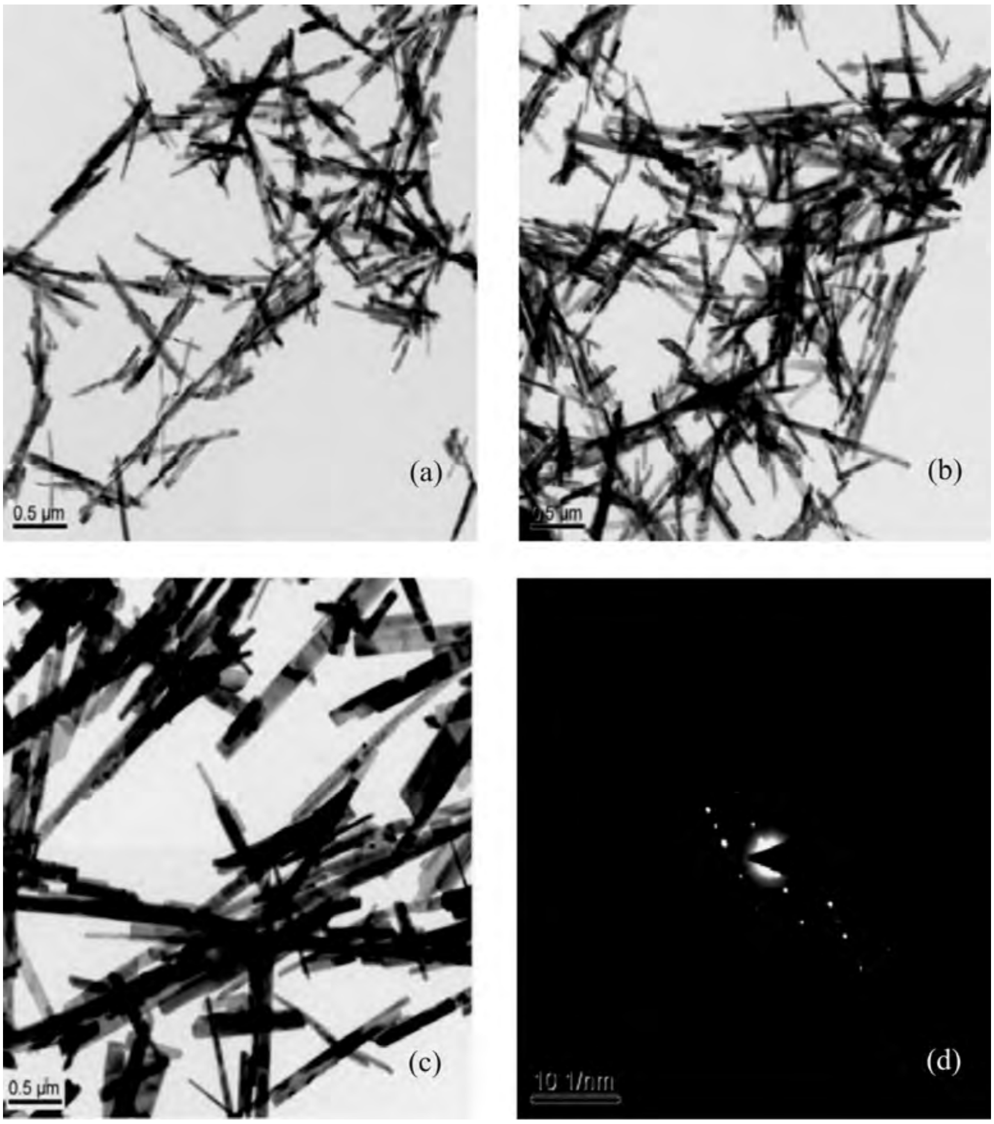

Figure 2 (**a**)–(**c**) TEM images of the $CdWO_4$ nanorods prepared with an SDBS concentration of 0.005, 0.01 and 0.015 mol L^{-1}, respectively (pH = 7). (**d**) Selected area electronic diffraction (SAED) pattern of an single $CdWO_4$ nanorod.

The TEM images of a single $CdWO_4$ nanorod synthesized at pH value of 5, 7 and 9, respectively, are shown in Figs. 3a, 3b and 3c (0.01 mol L^{-1} SDBS). The inset of each image is the HRTEM lattice diagram of a part of the nanorod. The widths of the $CdWO_4$ nanorods synthesized at three different pH values are all about 55 nm, which implies that pH does not bring about significant changes in the morphology of the $CdWO_4$ nanorods. However, the pH value does impacts on crystallinity of the $CdWO_4$ nanorods. It can be seen from the insets that the $CdWO_4$ nanorod synthesized with at a pH of 7 has the best crystallinity and almost no lattice defects. The nanorods obtained at pH = 5 and 9 have relatively poor crystallinity, with many line defects (the white arrows in the insets in Figs. 3a and 3c). The crystallinity of $CdWO_4$ nanorod prepared in acidic environment (pH = 5) is poorer than that in alkaline (pH = 9) and neutral (pH = 7) solutions. This is consistent with the XRD results.

The elemental identification of the synthesized product was obtained with an energy dispersive X-ray spectrometer (EDX) attached to the TEM system. Figure 4 is the EDX spectrum of an individual $CdWO_4$ nanorod.

It can be seen from the diagram, in addition to signals of Cd, W and O, Signal C originates from the TEM grid. EDX spectrum of an optional individual $CdWO_4$ nanorod at 180 °C for 24 h with the SDBS concentration of 0.01 mol L^{-1} (pH = 7). The C signal comes from the TEM grid. Quantitative analysis shows that atomic number ratio of the elements of Cd, W and O is approximately 1:1:4 and is consistent with the composition of $CdWO_4$, indicating that the synthetic products are $CdWO_4$ crystal.

PL spectra were measured at room temperature on a steady-state fluorescence and a phosphorescence lifetime spectrometer with an excitation wavelength of 320 nm. A steady-state Xe-arc lamp with an output power of 450 W was employed as excitation source. The PL spectra of the $CdWO_4$ nanorods at pH = 5, 7 and 9 (0.01 mol L^{-1} SDBS) are shown in Fig. 5. A strong blue-green emission band is present in the 400–600 nm range in all three spectra in which there are a strong emission peak at 485 nm and a shoulder at 460 nm. Compared to the PL emission (460 nm) of a massive $CdWO_4$ single crystal,[17] the strongest emission peak position of the $CdWO_4$ nanorods has a red shift of 25 nm. Here, it is noteworthy that the emission peak is also influenced by the excited wavelength,[18] size and aspect ratio of the $CdWO_4$ crystallites.[19] The PL spectra also demonstrate that the intensities of the PL emissions of the $CdWO_4$ nanorods prepared at different pH values are variable. The intensity of the $CdWO_4$ nanorods prepared with pH 7 is highest and at pH 5 is lowest. By comparing the TEM results, we can see a transformation of the lumines-

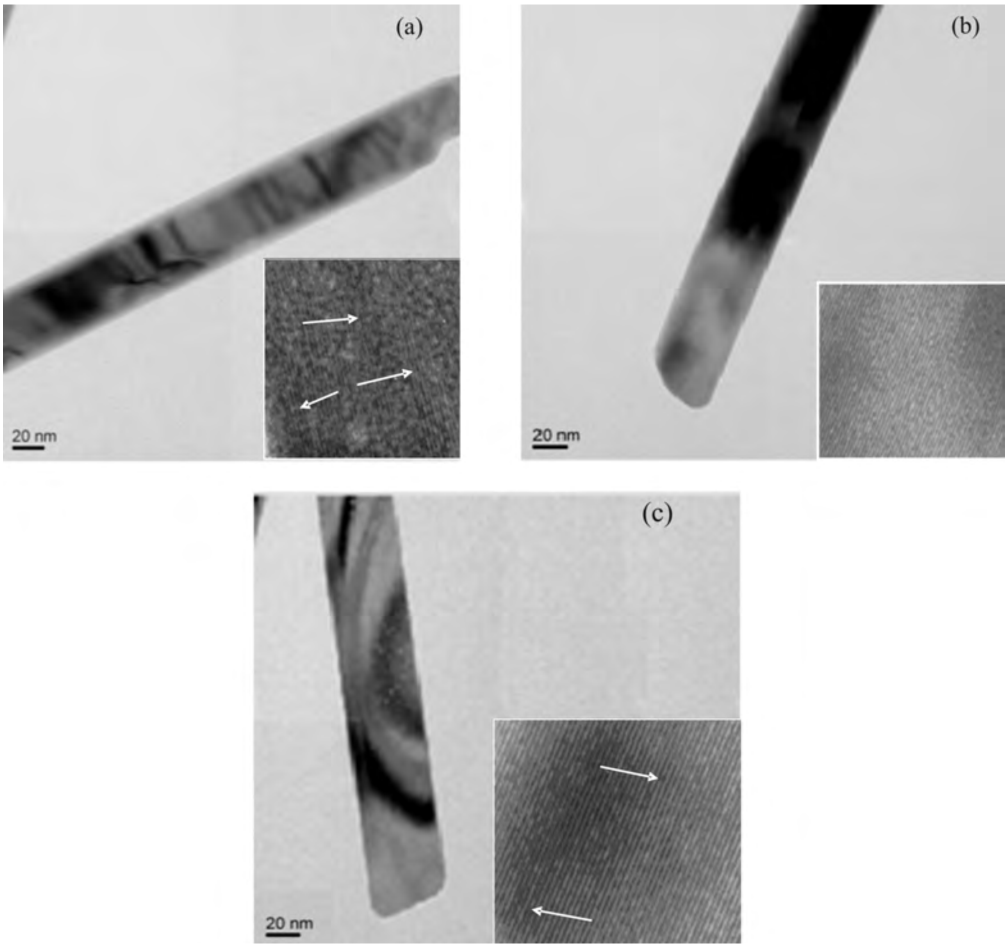

Figure 3 TEM images of a randomly chosen $CdWO_4$ nanorod synthesized with PH = 5, 7 and 9, respectively. The inset in each image is the HRTEM lattice diagram of a part of the nanorod.

cence intensity of the $CdWO_4$ nanorods synthesized at different pH values. This indicates that the PL emission intensity of the $CdWO_4$ nanorods is associated with the crystallinity of the products. Fluorescence emission originates from a recombination of electron-holes. Low emission intensity means that light-emitting material has a low recombination rate of electron-holes and a high separation rate of electron-holes. Consequently, the fluorescence intensity of the $CdWO_4$ nanorods increases with the crystallinity of the samples. At the same time, the high-energy peak at 322 nm, in the UV light zone, is present

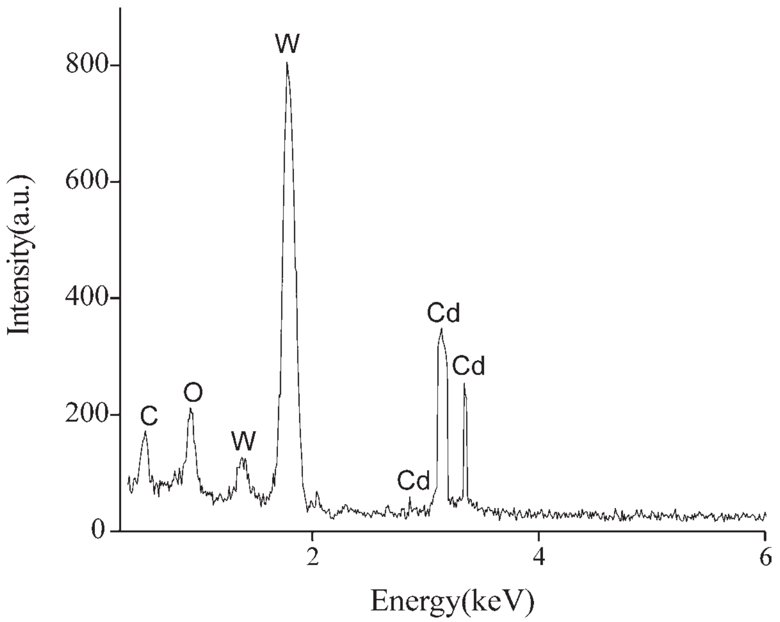

Figure 4 EDX spectrum of an optional individual $CdWO_4$ nanorod at 180 °C for 24 h with the SDBS concentration of 0.01 mol L^{-1} (pH = 7). The C signal comes from the TEM grid.

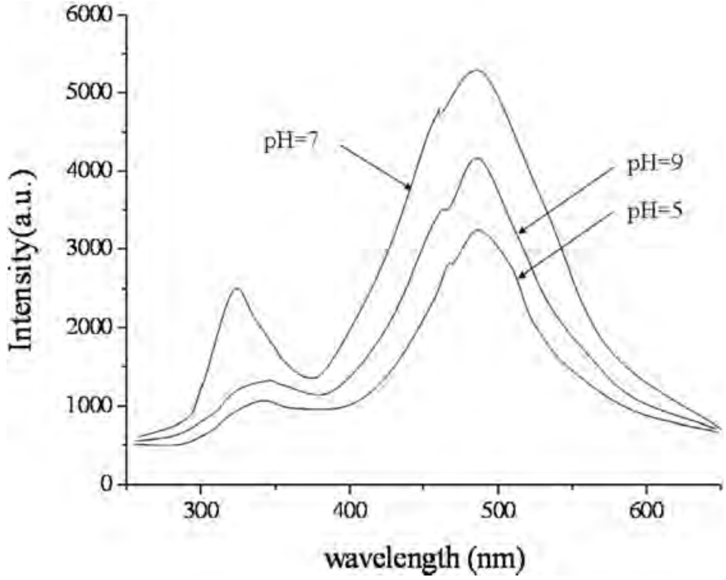

Figure 5 Room temperature PL spectra of the $CdWO_4$ nanorods synthesized at different pH values.

in the PL spectrum of the $CdWO_4$ nanorods obtained at pH 7 due to its good crystallinity.[20] The peak is possibly a band edge ultraviolet emission. The visible emission is usually ascribed to structural defects (surface oxygen vacancies).[21,22] The UV emission is attributed to the near-band-edge emission and arises from the recombination of free excitons through an exciton-exciton collision process[23]. Chen and coworkers attribute the band edge UV emission to the radiative recombination of excitons bound to neutral donor.[24]

The PL spectra of the $CdWO_4$ nanorods prepared with an SDBS concentration of 0.005, 0.01 and 0.015 mol L^{-1}, respectively, are shown in Fig. 6 (pH = 7). The ranges of fluorescence emission band (400–600 nm), as well as the positions of the strong emission (485 nm) and shoulder peaks (460 nm), are almost identical in all three spectra. The high-energy peaks at 322 nm, in the UV light zone, are present in the three spectra. The results indicate that the PL spectra of the well-crystallized $CdWO_4$ nanorods show, not only a strong blue-green emission band, but a band edge UV emission. Meanwhile, it can be seen from Fig. 6 that the intensity of the PL emission of the $CdWO_4$ nanorods synthesized with an SDBS concentration of 0.01 mol L^{-1}, is a maximum.

The change in PL emission intensity can be attributed to a one-dimensional confinement effect, and be caused by the differences in morphology of the $CdWO_4$ nanorods. The trend is in agreement with the change in aspect ratio of the $CdWO_4$ nanorods. These results suggest that the intensity of PL emission is strongly bound up with the morphology of the $CdWO_4$ nanorod powders.

From the above results, we can see that the pH value and concentration of surfactant SDBS do not affect the position of blue-green band in the 400–600 nm range. However, the luminescence intensity of blue-green emission bands of the $CdWO_4$ nanorods varies with pH and SDBS concentration. Previously, this luminescence was attributed to electronic transition within the coordination anion of WO_6^{6-} ref. 25. The PL emission bands were ascribed to the $^1A_1 \rightarrow {}^3T_1$ transition within the WO_6^{6-} complex.[26] We believe that the photoluminescence properties depend strongly on the morphology and crystallinity of the $CdWO_4$ nanorods.

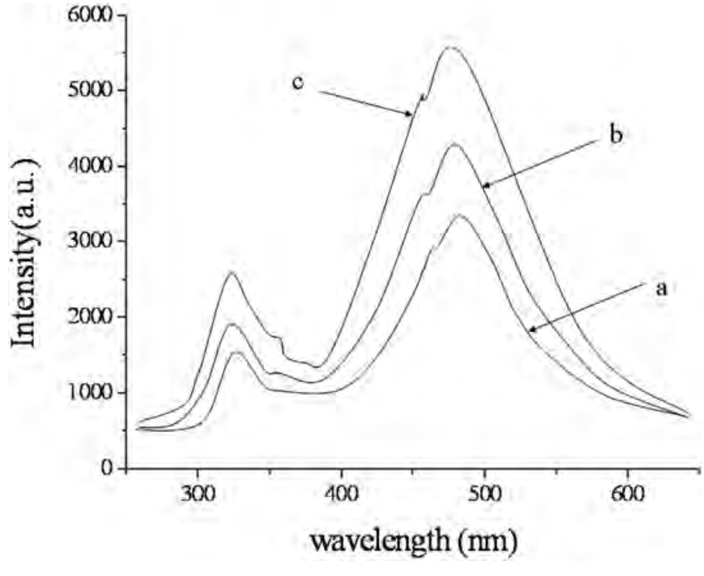

Figure 6 PL spectra of the $CdWO_4$ nanorods prepared with an SDBS concentration of (a) 0.005 (b) 0.015 and (c) 0.01 mol L^{-1}, respectively.

4. Conclusions

$CdWO_4$ nanorods were synthesized by a hydrothermal method using $Na_2WO_4 \cdot 2H_2O$ and $CdCl_2 \cdot 2.5H_2O$ as raw materials in the presence of the surfactant SDBS. The lengths and widths of the $CdWO_4$ nanorods fall into the range of 0.8–2.5 μm and 50–250 nm, respectively. The results show that the surfactant plays the roles of a soft template and an adsorbent of crystal face oriented growth in the formation of the nanorods. The surfactant concentration and pH value impact on the morphology and crystallinity of the $CdWO_4$ nanorods. The intensity of photoluminescence increases with the crystallinity and aspect ratio of the $CdWO_4$ nanorods.

Acknowledgements

This work was supported by the National Nature Science Foundation (51172187), the SPDRF (20116102130002) and 111 Program (B08040) of MOE, Xi'an Science and Technology Foundation (CX1261-2) of China.

References

1 S.J. Chen, J.H. Zhou, X.T. Chen, J. Li, L.H. Li, J.M. Hong, Z. Xue and X.Z. You, *Chem. Phys. Lett.*, 2003, **375**, 185–190.

2 S. Kwan, F. Kim, J. Akana and P.D. Yang, *Chem. Commun.*, 2001, **5**, 447–448.

3 B. Liu, S.H. Yu, L.J. Li, F. Zhang, Q. Zhang, M. Yoshimura and P.K. Shen, *J. Phys. Chem. B,* 2004, **108**, 2788–2792.

4 X.L. Hu and Y.J. Zhu, *Langmuir,* 2004, **20**, 1521–1523.

5 H.W. Liao, Y.F. Wang, X.M. Liu, Y.D. Li and Y.T. Qian, *Chem. Mater.*, 2000, **12**, 2819–2821.

6 V.G. Bondar, S.F. Burachas, K.A. Katrunov, V.P. Martinov, V.D. Ryzhikov, V.I. Manko, H.H. Gutbrod and G. Tamulaitis, *Nucl. Instr. Meth. Phys. Res. A,*1998, **411**, 376–382.

7 L. Grigorjeva, R. Deych, D. Millers and S. Chernov, *Radi. Measure.,* 1998, **29**, 267–271.

8 A.P. Chichagov, V.V. Iliukhin and N.V. Belov, *Sov. Phys. Dokl.,* 1966, **11**, 11–13.

9 C.D. Greskovich, D. Cusano, D. Hoffman and R.J. Riedner, *Am. Ceram. Soc. Bull.,* 1992, **71**, 1120–1126.

10 S.C. Sangeetas and Sangeeta, *J. Cryst. Growth,* 1999, **200**, 191–198.

11 Y.G. Wang, J.F. Ma, J.T. Tao, X.Y. Zhu, J. Zhou, Z.Q. Zhao, L.J. Xie and H.Tian, *Mater. Sci. Eng. B,* 2006, **130**, 277–281.

12 R. Dafinova, K. Papazova and A. Bojinova, *J. Lumin.*, 1997, **75**, 51–55.

13 K. Tanaka and D. Sonobe, *Appl. Surf. Sci.*, 1999, **140**, 138–143.

14 Z.D. Lou, J.H. Hao and M. Cocivera, *J. Lumin.,* 2002, **99**, 349–354.

15 K. Lennstrom, S.J. Limmer and G.Z. Cao, *Thin Solid Films,* 2003, **434**, 55–61.

16 Y.G. Wang, J.F. Ma, J.T. Tao, X.Y. Zhu, J. Zhou, Z.Q. Zhao, L.J. Xie and H. Tian. *J. Am. Ceram. Soc.,* 2006, **89**, 2980–2982.

17 V.A. Pustovarov, A.L. Krymov and B. Shulgin, *Rev. Sci. Instrum.,* 1992, **63**, 3521–3523.

18 M.M. Chirilaa, K.T. Stevens, H.J. Murphy and N. C. Gilesa, *J. Phys. Chem. Solids,* 2000, **61**, 675–679.

19 H.W. Liao, Y.F. Wang, X.M. Liu, Y.D. Li and Y.T. Qian, *Chem. Mater.,* 2000, **12**, 2819–2821.

20 J.H. Yang, D.D. Wang, L.L. Yang, Y.J. Zhang, G.Z. Xing, J.H. Lang, H.G. Fan, M. Gao and Y.X. Wang, *J. Alloys Compd.,* 2008, **450**, 508–511.

21 J.H. Yang, J.H. Lang, L.L. Yang, Y.J. Zhang, D.D. Wang, H.G. Fan, H.L. Liu, Y.X. Wang and M. Gao, *J. Alloys Compd.,* 2008, **450**, 521–524.

22 D.D. Wang, J.H. Yang, L.L. Yang, Y.J. Zhang, J.H. Lang and M. Gao, *Cryst. Res. Technol.,* 2008, **43**, 1041–1045.

23 Y.C. Kong, D.P. Yu, B. Zhang, W. Fang and S.Q. Feng, *Appl. Phys. Lett.,* 2001, **78**, 407–409.

24 R. Chen, G.Z. Xing, J. Gao, Z. Zhang, T. Wu and H.D. Sun, *Appl. Phys. Lett.,* 2009, **95**, 061908–061910.

25 Y.A. Hizhnyi, S.G. Nedilko and T.N. Nikolaenko, *Nucl. Instrum. Methods Phys. Res. A,* 2005, **537**, 36–39.

26 K. Polak, M. Nikl, K. Nitsch, M. Kobayashi, M. Ishii, Y. Usuki and O. Jarolimek, *J. Lumin.,* 1997, **781**, 72–74.